Supplementary Information

Nitrogen-Doped Carbon Layer Thickness Modulates Cu^0/Cu^+ Interface for Selective and Stable CO_2 Electroreduction to Ethylene

Jvwei Liu[a], Qiang Zhang[*a,b], Shenjie Zhang[a], Conglin Chen[a], Jiaxin Jiang[a], Yayun Luo[a], Weiming Yang[a], Junqiang Xu[c]

a School of Chemistry & Chemical Engineering, Chongqing University of Technology, Chongqing 400054, P. R. China.

b National Engineering Laboratory for Methanol to Olefins, Dalian National Laboratory for Clean Energy, iChEM (Collaborative Innovation Center of Chemistry for Energy Materials), Dalian Institute of Chemical Physics, Chinese Academy of Sciences, Dalian 116023, P. R. China.

c Yangtze Normal University, Chongqing 408100, P. R. China.

**Corresponding authors: School of Chemistry & Chemical Engineering, Chongqing University of Technology, Chongqing 400054, P. R. China.*

E-mail addresses: zqiang@cqut.edu.cn (Qiang *Zhang)*

Mailing address for correspondence:

Dr. Zhang, Qiang (Prof.)

School of Chemistry & Chemical Engineering, Chongqing University of Technology, No.66 Hongguang Rd., Banan, Chongqing 400054, China

Tel: +86-23-625678923

Fax: +86-23-625678923

E-mail: zqiang@cqut.edu.cn

1. Experimental

1.1. Synthesis of Cu_2O

The steps to synthesize Cu_2O were as follows: First, 0.025 mmol of copper acetate monohydrate was weighed into 250 mL of diethylene glycol (DGE), and the mixture was added to a three-necked flask. The flask was heated to 160 °C with magnetic stirring under condensation reflux and held for 1 h. After the reaction, the heat source was removed and the flask was naturally cooled to room temperature. The reaction solution was centrifuged at 2000 $r \cdot min^{-1}$ for 30 min, the precipitate was collected and washed five times with ethanol. The residue was dried in a vacuum oven at 90°C for 4 h to obtain Cu_2O nanoparticles.

1.2. Synthesis of Cu_2O@ZIF-8

In a typical experiment, the prepared Cu_2O nanoparticles and 1.000 g PVP were dispersed in 20 mL methanol solution and sonicated for 5 min. Then, 20 mL methanol solution containing 0.700 g $Zn(NO_3)_2 \cdot 6H_2O$ and 0.250 g PVP and another equivalent volume of methanol solution of 2-methylimidazole (0.260 g 2-methylimidazole, 0.250 g PVP) were successively introduced. Next, the resulting mixture was stirred at room temperature for 24 hours. After the reaction, the powder was collected by centrifugation and washed 3 times with methanol. At last, the synthesized sample was dried in a vacuum oven at 60 °C for 12 h.

1.3. Synthesis of Cu^0/Cu^+@C-N

The obtained Cu^0/Cu^+@C-N was calcined by Cu_2O@ZIF-8 at 1200 °C for 3 h under NH_3 atmosphere. The average heating rate was 5 °C min^{-1}. Cu^0/Cu^+@C-N-3.6 and Cu^0/Cu^+@C-N-5.4 and Cu^0/Cu^+@C-N-8.8 were prepared using the same method, differing only in the amount of PVP used, which was 1.000 g, 3.000 g, and 5.000 g respectively.

1.4. Synthesis of Cu

The obtained Cu was calcined by Cu_2O NPs at 200 °C for 2 h under an H_2 atmosphere. The average heating rate was 5 °C min^{-1}.

1.5. Characterization

The crystal structure of the samples was characterized by X-ray diffraction (XRD) diffractometer (Rigaku D/max-3C) equipped with a graphite monochromator for Cu Ka (40 kV, 40 mA, k = 1.542 Å) with a scan speed of 5°min^{-1} and a scan range of 2θ = 10°-90°. The morphology of the samples was observed with a scanning electron microscope (SEM, JSM-7800F). The structure and elemental content of the catalysts were examined using transmission electron microscopy (TEM) and energy-dispersive x-ray spectroscopy (EDX). The elemental composition of the catalyst surface was determined using X-ray photoelectron spectroscopy (XPS, ESCALAB250Xi) under Al-Kα (15 KV, 30 mA). Raman spectra were recorded on a Renishaw RM-3000 Micro-Raman system.

1.6. Electrochemical measurements

CO_2RR was carried out in a standard three-electrode system using 0.1 M $KHCO_3$ solution (298 K, pH = 6.8) as electrolyte in an airtight two-chamber electrochemical cell (Nafion-212 membrane separation). The counter electrode used in the experiment was a platinum electrode; the reference electrode was a calomel electrode; the working electrode was a glassy carbon electrode; and the electrochemical workstation was CHI-660E. First, catalyst (0.040 g) and Nafion solution (5 wt%, 5 μL) were added to isopropanol (395 mL) and sonicated for 10 min to obtain the catalyst slurry. To ensure uniform catalyst dispersion, linear sweep voltammetry (LSV) results comparing different ultrasonication durations (Fig. S5) revealed that 10-minute treatment yielded higher current density and enhanced electrochemical activity, confirming the catalyst's uniform dispersion. Conversely, excessively prolonged ultrasonication may induce structural changes in the catalyst, thereby diminishing electrochemical activity. Then it was evenly dripped onto the surface of the glassy carbon electrode (area = 0.07 cm^2) and dried naturally to obtain the working electrode. The electrolyte was purged by high-purity argon (99.999%) for 30 min to remove the impurity gas, and then high-purity CO_2 (99.99%) was injected into the electrolyte to form a saturated CO_2 solution. The catalytic activity of the

catalyst was evaluated by cyclic voltammetry (CV) and linear sweep voltammetry (LSV). The stability of the catalyst was analyzed by chronoamperometry. The electrochemical impedance of the catalyst was analyzed by electrochemical impedance spectroscopy (EIS, frequency 1-10^6 Hz, potential -1.0 V vs. RHE, amplitude 5 mV). The electrode potentialswere converted into reversible hydrogen electrode by the equation:

E (vs. RHE) = E (vs. Hg/Hg_2Cl_2) + 0.241 V + 0.059 × pH

1.7. Product Analysis

The gaseous products were detected by a gas chromatograph (SC3000B) equipped with a TDX01 molecular sieve column at 30-minute intervals. The composition of the liquid sample was analyzed by nuclear magnetic resonance (NMR) spectroscopy. Sample preparation for NMR: 0.1 mL D_2O containing 0.05 mL dimethyl sulfoxide was used as the internal standard liquid. After the electrolytic reaction, the electrolyte of 0.1 mL was mixed with the internal standard solution for NMR detection. Faraday efficiency and conversion frequency are calculated by measuring the product and current value of the reaction at constant potential for 2 h. Faradaic efficiency (FE) of gaseous products at each applied potential was calculated based on the equation:

$$FE_{C2H4} = \frac{z \times P \times F \times V \times v_i}{R \times T \times J}$$

Partial current density for C_2H_4 product normalized by the geometrical electrode area ($J_{C2\ products}$, A cm^{-2}) was determined by calculating the total current density multiplied by FE of C_2H_4 product: $J_{C2H4product} = FE_{C2H4product} \cdot J$. C_2H_4 product mass activity was determined by C_2H_4 product partial current density divided by catalyst mass on the electrode: Mass activity= $\frac{J_{C2H4product}}{m}$. C_2H_4 product production rate normalized by the geometrical electrode area (n, mol·cm^{-2}·h^{-1}) was calculated based on the formula: n = $\frac{P \times V \times v_i}{R \times T}$ ×3600. Where z is the number of electrons transferred per mole of gas product (z is 12 for C_2H_4 product), F is Faraday constant

(96500 C·mol^{-1}), P is pressure (1.01×105 Pa), V is the gas volumetric flow rate (3.33×10 7 m^{3}·s^{-1}), v_i is the volume concentration of gas product determined by GC, T is the temperature (298.15K), R is the gas constant (8.314 Jmol^{-1}·K^{-1}), J is the steady-state current at each applied potential (A), m is the catalyst mass on the electrode (g·cm^{-2}).

1.8. Density functional theory calculation

The CASTEP was used to perform plane-wave density functional theory (DFT) calculation. Ultrasoft potentials (USP) were employed to describe electron-ion interaction. The Perdew-Burke-Ernzerhof (PBE) formulation of the generalized gradient approximation (GGA) and the DFT-D2 method proposed by Grimme were employed to account for electron-electron interactions and Vander Waals forces. The Brillouin zone integral was calculated using 3×3×1 k-point grid generated by the Monkhorst-Pack (MP) scheme. The cutoff kinetic energy was set at 400eV. The convergence limit for the electronic self-consistent field loop was 1×10^{6} eV · atom1. The residual force on the atomic structure was minimized to be below 0.03 eV. The cell parameters were optimized using the finite basis correction method until the stress was less than 0.05 GPa. The positions of all atoms were fully relaxed without any symmetry constrains.

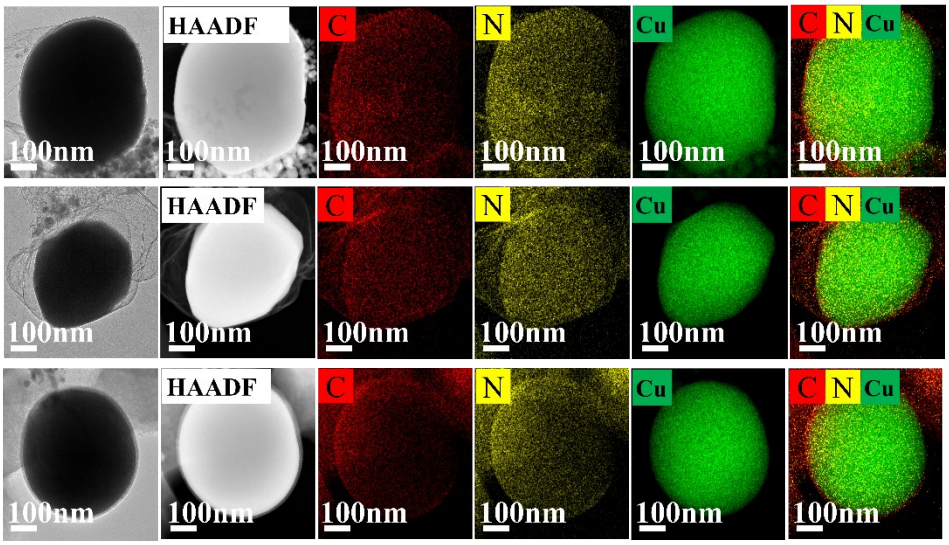

Fig. S1. TEM and elemental mapping images of Cu@C-N.

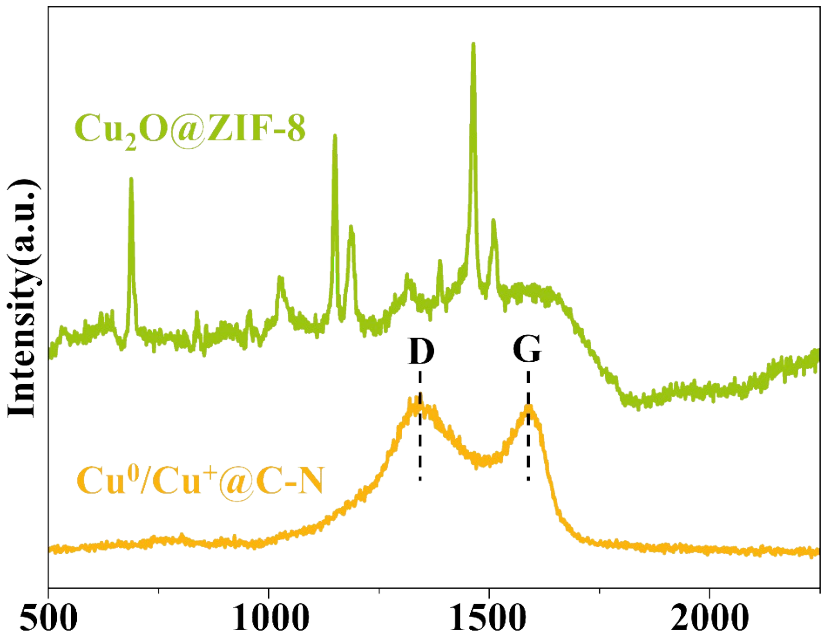

Fig. S2. Raman patterns of Cu_2O@ZIF-8 and Cu^0/Cu^+@C-N.

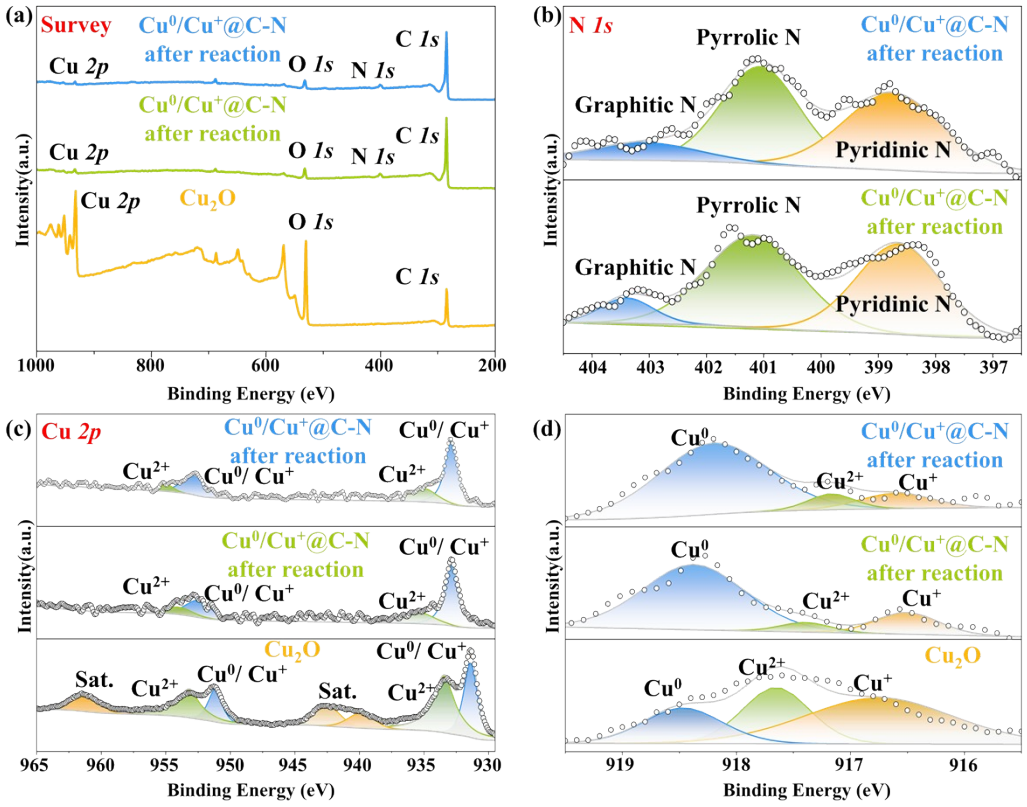

Fig. S3. (a) the XPS full survey of Cu_2O, Cu^0/Cu^+@C-N before reaction, and Cu^0/Cu^+@C-N after reaction. (b) N *1s* spectra of Cu^0/Cu^+@C-N before reaction, and Cu^0/Cu^+@C-N after reaction. (c) Cu *2p* spectra of Cu_2O, Cu^0/Cu^+@C-N before reaction, and Cu^0/Cu^+@C-N after reaction. (d) Cu *LMM* spectra of Cu_2O, Cu^0/Cu^+@C-N before reaction, and Cu^0/Cu^+@C-N after reaction.

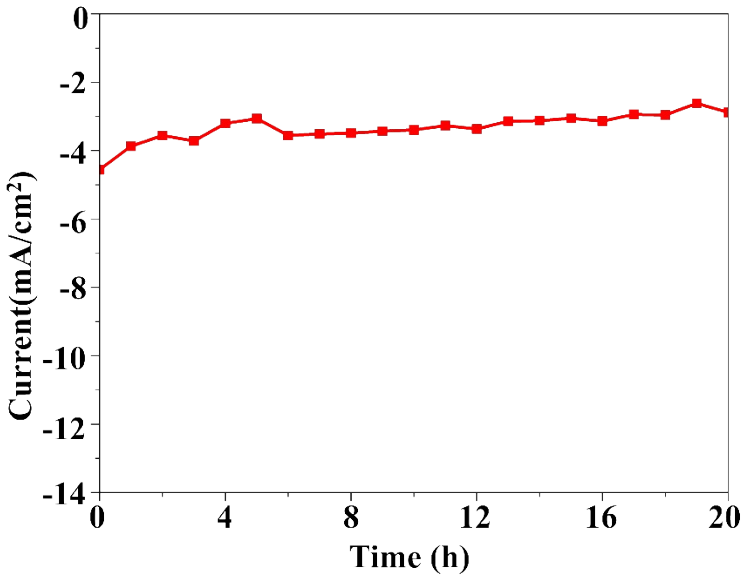

Fig. S4.Chronoamperometry curves of Cu^0/Cu^+@C-N.

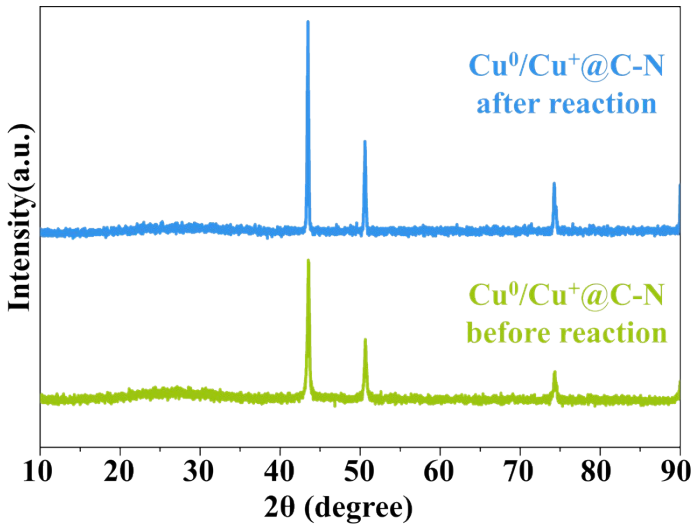

Fig. S5. XRD patterns of Cu^0/Cu^+@C-N before reactionand Cu^0/Cu^+@C-N after reaction.

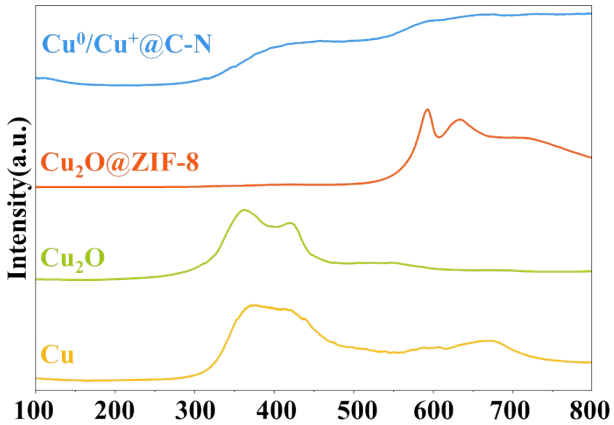

Fig. S6.CO_2-TPD curves of Cu, Cu_2O, Cu_2O@ZIF-8, and Cu_0/Cu^+@C-N.

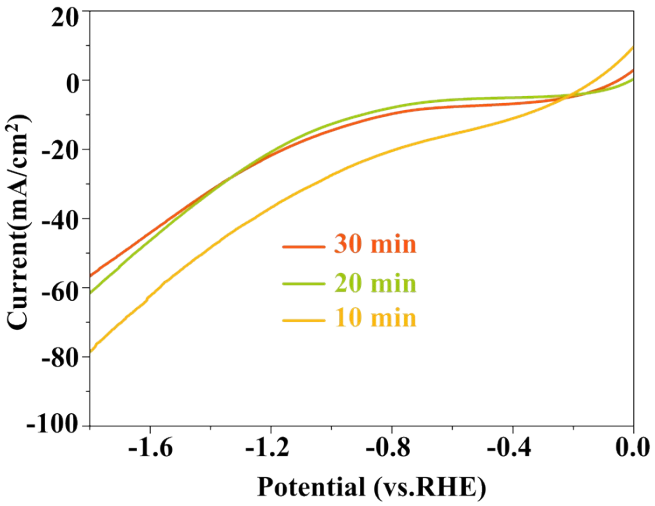

Fig. S7. LSV curves at different ultrasonic treatment times

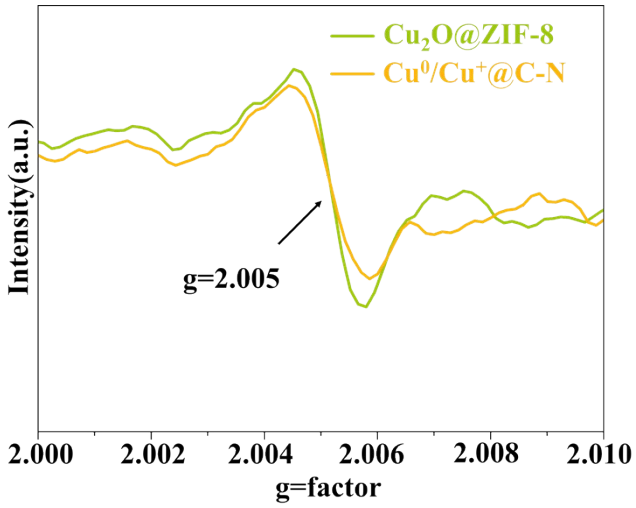

Fig. S8. EPR spectra of Cu_2O@ZIF-8 and Cu^0/Cu^+@C-N

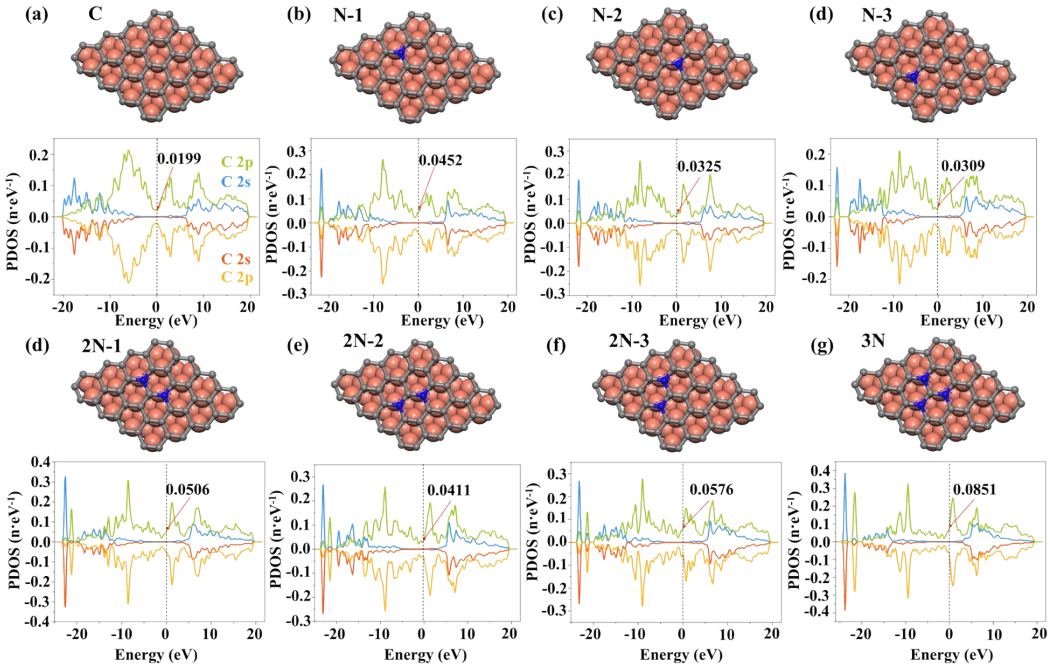

Fig. S9 Partial density of states of the different N doped concentrations and N doping types.

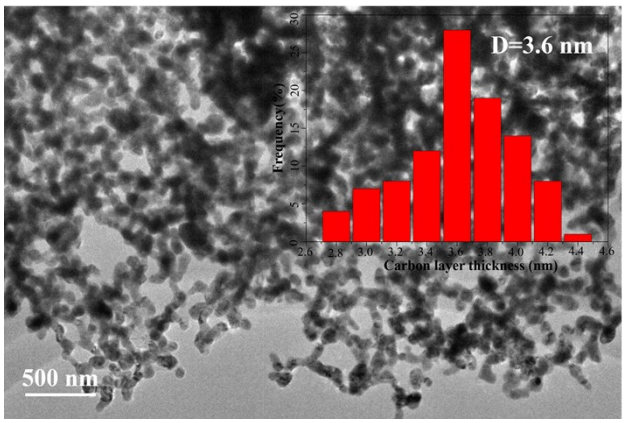

Fig. S10 The thickness distribution of Cu^0/Cu^+@C-N-3.6.

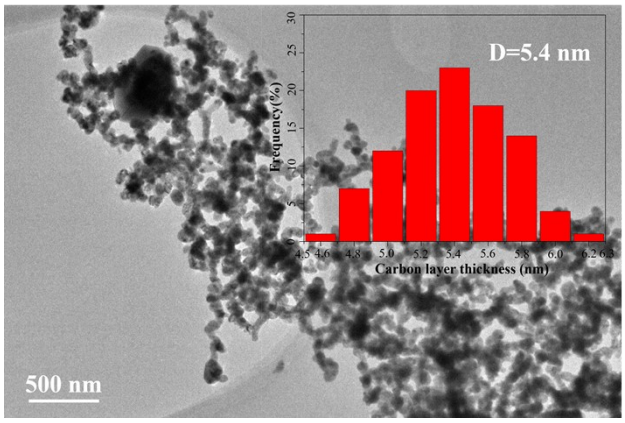

Fig. S11 The thickness distribution of Cu^0/Cu^+@C-N-5.4.

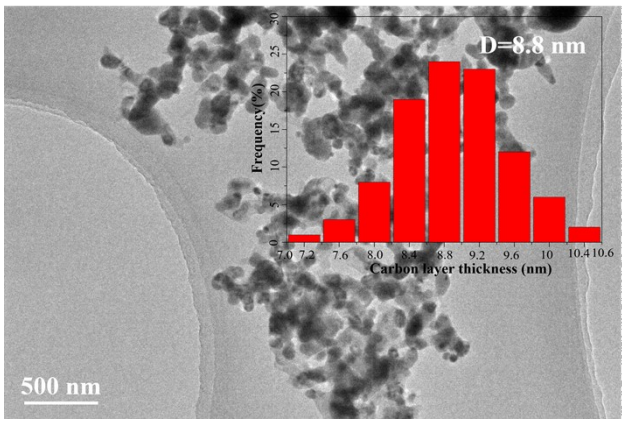

Fig. S12 The thickness distribution of Cu^0/Cu^+@C-N-8.8.

Table S1. The Chemical states of Cu in Cu_2O, Cu^0/Cu^+@C-N before reaction, and Cu^0/Cu^+@C-N after reaction

Chemiacal state	Cu^0	Cu^+	Cu^{2+}
Cu_2O	28.10%	51.02%	20.88%
Cu^0/Cu^+@C-N before reaction	73.56%	16.18%	10.26%
Cu^0/Cu^+@C-N after reaction	78.38%	14.63%	6.99%

Table S2 Catalytic performance of CO_2 activation via electrochemical strategy.

Name	Applied Potential	Electrolyte	Time (h)	FE_{C2H4} (%)	current density ($mA \cdot cm^{-2}$)	Ref.
Cu/Me-COF	-1.2 V vs RHE	1 M KOH	89.6	46.8	374.2	[1]
Ga–Cu_2O	-1.3 V vs RHE	0.5 M $KHCO_3$	50	26.4	33	[2]
Cu2O Nano-Homojuncti	-1.4 V vs RHE	0.1 M K_2SO_4	200	73.7	38.2	[3]

on						
In/Cu		0.1 M $KHCO_3$	1500	85	750	[4]
n-Cu Nanosheets	-1.18 V vs RHE	0.1 M K_2SO_4	14	83.2	60	[5]
De-Au_1Cu SAA	-1.0 V vs RHE	1 M KOH	54	52	252	[6]
$Cu_2Y_2O_5$	-1.0 V vs RHE	1 M KOH	10	70	200	[7]
This work	1.7 V vs. RHE	0.1 M KOH		88.4	8.7	

Table S3. CO_2 Adsorption Capacity

Catalysts	Cu	Cu_2O	Cu_2O@ZIF-8	Cu^0/Cu^+@C-N
CO_2 Adsorption Capacity（$mmol \cdot g^{-1}$）	15.8019	23.3083	46.6624	47.5215

[1] Z. Qian, Y. Liu, Z. Lin, N. Ye, Y. Tan, F. Liu, Y. Gu, Q. Huang, H. Guo, M. Luo and S. Guo, *J. Am. Chem. Soc.*, 2025, **147**, 21877-21884.

[2] W. Ren, G. Wang, F. Zhang, J. Wang, K. Ji, X. Wang, X. Li, J. Yang, R. Liu, Y. Ji, S. Wang, Z. Chen, B.-J. Ni, J. Xie, Z. Yang and Y.-M. Yan, *ACS Appl. Mater. Interfaces.*, 2025, **17**, 50794-50804.

[3] R. Zhang, J. Zhang, Y. Song, Y. Yang, M. Li, Y. Zhao, Y. Teng, B. Han and Z. Chen, *Angew. Chem. Int. Ed.*, 2025, **64**, e202501554.

[4] L. Huang, G. Gao, J. Zhao, W.L. Roberts and X. Lu, *Nat. Catal.*, 2025, **8**, 968-976.

[5] B. Zhang, J. Zhang, M. Hua, Q. Wan, Z. Su, X. Tan, L. Liu, F. Zhang, G. Chen, D. Tan, X. Cheng, B. Han, L. Zheng and G. Mo, *J. Am. Chem. Soc.*, 2020, **142**, 13606-13613.

[6] Y. Zhao, Y. Wang, Z. Yu, C. Song, J. Wang, H. Huang, L. Meng, M. Liu and L. Liu, *ACS Nano.*, 2025, **19**, 4505-4514.

[7] J. Lu, M. Xia, J. Liang, L. Zou, X. Liang, Y. Gao, F. Li, J. Gao and J. Liu, *Chem. Eng. J.*, 2025, **506**, 160284.